analytical chemistry

ARTICLE

pubs.acs.org/ac

Dating Archeological Lead Artifacts from Measurement of the Corrosion Content Using the Voltammetry of Microparticles

Antonio Doménech-Carbó,*[,†] María Teresa Doménech-Carbó,[‡] and María Amparo Peiró-Ronda[§]

[†]Departament de Química Analítica, Universitat de València, Dr. Moliner 50, 46100 Burjassot (València), Spain

[‡]Institut de Restauració del Patrimoni, Universitat Politécnica de València, Camino de Vera 14, 46022 València, Spain

[§]Museu de Prehistòria de València, Corona 36, 46003 València, Spain

Supporting Information

ABSTRACT: A methodology for dating archeological lead artifacts based on the voltammetry of microparticles is described. This methodology is based on the comparison of the height of specific voltammetric features from PbO_2 and PbO corrosion products formed under long-term alteration conditions. Calibration of the method was performed with the help of a series of well-documented lead pieces from the funds of different museums of the Comunitat Valenciana (Spain) covering from the fifth century B.C. to present day. The variation of peak currents with the time of corrosion can be fitted to the same potential rate law as that found by Reich ($\alpha = 0.070 \pm 0.005$), using measurements on the Meissner fraction in the superconducting state of lead. The proposed electrochemical methodology enables the dating of archeological lead artifacts with a time-dependent uncertainty estimated to be ±150 years for the most ancient samples in this study.

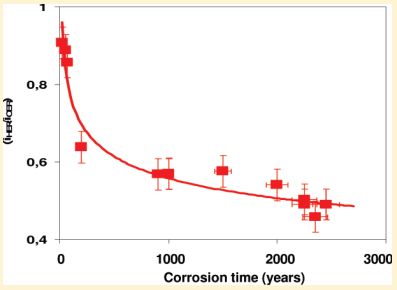

The dating of metal artifacts is an important analytical target in archaeometric studies. Radiocarbon, the uranium−lead radioactive series, and luminescence analysis are the main techniques used for absolute dating.[1,2] In this context, although iron artifacts occasionally were dated by the ^{14}C method performed on the traces of charcoal found in those objects, dating procedures for archeological artifacts made of copper, iron, tin, gold, or lead do not exist.[3] In addition to the methods listed above, chemical evaluation of the extent of corrosion in archeological artifacts can provide insight into the duration of the corrosion process by using several simplifying assumptions. This is the case of the obsidian method developed by Friedman and Smith for dating ceramics.[4] Reich et al.[3] used measurements on the Meissner fraction in the superconducting state of lead to evaluate the mass of the uncorroded metal in the sample in order to estimate the age of the archeological lead artifacts.

In this report, we present a procedure for dating archeological lead artifacts based on the numerical variation of specific features in the voltammetric response of sample-modified graphite electrodes immersed into aqueous electrolytes. As an antecedent, Scholz et al.[5] proposed a method for dating based on the electrochemical monitoring of the generation of point defects in ceramic materials. In this report, the voltammetry of microparticles (VMP) methodology is used. This technique, developed by Scholz et al.,[6,7] can be used for obtaining qualitative and quantitative information from samples of works of art.[8,9] Using a "graphite pencil" variant of VMP,[10,11] an essentially noninvasive analysis can be performed on a few nanograms of sample.

Lead was used widely in antiquity. Initially, it was mainly devoted to silver extraction via cupellation procedures, but since the Iron Age, lead has been produced for fishing nets, anchors, sling bullets, fastening iron clamps in the walls of buildings, water pipes, jewelry, and cult figures.[12,13] Lead metal offers a significant resistance to corrosion in many environments when it is exposed to the atmosphere, soil, fresh water, and seawater as a result of the formation of relatively insoluble films of primary corrosion products in the initial stages of exposure, which then protect it from further attack.

The corrosion products of lead offer well-defined electrochemical responses under VMP conditions.[14−17] In previous reports, we described the use of specific voltammetric signatures for the authentication of archeological lead[18] and the identification of corrosion products.[19] Here, the time variation of voltammetric signatures specifically attributed to PbO_2 (or possibly PbO_n ($1 < n < 2$)) and PbO species, formed during prolonged corrosion, is used for dating archeological lead artifacts. It should be noted that the interaction between the metal and the corrosion agents and pollutants results in chemical, electrochemical, or even biological corrosion processes, which can be accompanied by various pedological processes (recrystallization, segregation, desegregation, cementation, or monolithization) giving rise to a more or less complex patina of corrosion products. In general, one can distinguish between a primary patina, which is formed in the atmospheric environment during the usual handling of the piece, and a secondary patina, which is formed during the last

Received: March 25, 2011
Accepted: May 23, 2011

   dx.doi.org/10.1021/ac200731q | *Anal. Chem.* XXXX, XXX, 000–000

period of utilization or the initial stages of pedological processes. This can be accompanied by the patina of corrosion which results from processes of diffusion−segregation−deposition.[20]

Different specific VMP signatures from PbO_2 and PbO forming the corrosion layers of lead artifacts have been correlated with the corrosion time. These include the direct reduction signals for the different lead oxides in contact with an aqueous acetate buffer and the catalytic effects in the hydrogen evolution reaction (HER) and oxygen evolution reaction (OER) in contact with a phosphate buffer. It should be noted that the proposed methodology involves, as well as all other proposed dating methods,[1−5] samples whose composition and conditions of aging can be considered similar and that it requires calibration from well-documented samples accomplishing the above conditions.[1−5]

The application of the proposed methodology involves two main assumptions: (a) the corrosion process has occurred under quite similar conditions for all samples, and (b) corrosion proceeded uniformly through time. Calibration curves were obtained from a set of samples from the funds of the Prehistory Museum of Valencia, Archaeological Museum of Borriana, Museum of Montcada, and Bellas Artes Museum of Castelló (all from the Comunitat Valenciana, Spain), covering from the Iberian times (5th century B.C.) to contemporary time. Samples were selected from lead fragments (0.02−0.10 g) that were separated accidentally by the restorers from the original pieces during the process of extraction, cleaning, or conservative treatment of the archeological pieces. Such fragments are systematically conserved and catalogued by the archeologists and conservators of the museums. The original pieces were all found under burial conditions in the Comunitat Valenciana (Spain) in calcareous soils. Because of the corrosion processes often associated with restorative treatments and aggressive environments in museum cabinets,[21−23] only pristine archeological lead pieces were used for calibration. The selection of samples for time calibration was performed following these five criteria: (a) the lead artifacts corroded under burial conditions in chalk soils from a Valencian region; (b) litharge-based patination is present on the artifacts; (c) no cleaning or restorative treatments have been applied to the artificats; (d) the artifacts have not been exposed to corrosion in the museum environment; (e) there is unambiguous dating of the artifacts. The characteristics and dating of the studied samples of archeological lead can be found in the Supporting Information.

EXPERIMENTAL SECTION

The electrochemical experiments were performed with sample-modified graphite electrodes at 298 K in a conventional three-electrode cell under an argon atmosphere, using reagents and equipment described in the Supporting Information. The VMP experiments were performed at paraffin-impregnated graphite electrodes (PIGEs)[6,7] upon the mechanical transferring of a few nanograms of sample by means of the one-touch methodology already described.[19] Fragments (typically 10−20 mg) of the selected samples were used to modify graphite electrodes by placing them on an agate mortar and pressing the graphite bar on the lead fragments.

Samples include three contemporary pieces (S.1−S.3 in the Supporting Information) stored in university buildings, 14 genuine archeological samples (S.3−S.17), and three forgeries found in archeological sites (S.18−S.20). Calibration was performed with pristine, nonrestored archeological samples (S.3−S.6 and S.9−S.16). Archaeological samples S.7, S.8, and S.17, which were subjected to restoration/conservation procedures in recent times and, therefore, possess an altered patina, have also been tested but were not used for time calibration.

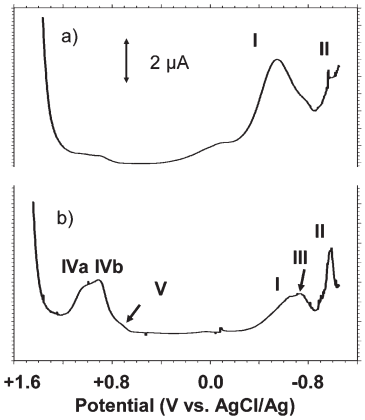

Figure 1. SWVs for graphite electrodes modified by means of the one-touch methodology for the following: (a) contemporary lead (S.1); (b) the Visigothic sample from the Punta de l'Illa (S.10) immersed into 0.50 M HAc/NaAc, pH 4.85. The potential scan was initiated at +1.45 V in the negative direction. The potential step increment was 4 mV; the square wave amplitude was 25 mV; and the frequency was 5 Hz.

RESULTS AND DISCUSSION

General Voltammetric Pattern. Figure 1 compares the voltammetric responses for (a) a contemporary patinated lead (S.1 in the Supporting Information) and (b) a genuine archeological sample from the Visigothic period (6th century A.D., sample S.10) when the potential is scanned from +1.45 V vs AgCl/Ag in the negative direction. For contemporary lead, a main reduction peak appears at −0.55 V (I) accompanied by a cathodic shoulder at −0.95 V (II), near the rising current for solvent discharge. For samples of archeological lead, these peaks are accompanied by a cathodic shoulder at −0.70 V (III) and preceded by overlapping peaks at +1.10 and +0.90 (IVa and IVb, respectively) and +0.75 V (V) while peak II becomes significantly enhanced.

To rationalize this response, it should be taken into account that lead passivation leads to a porous PbO layer, so that, depending on the size of these pores, thermodynamic and kinetic passivation mechanisms can occur.[24−28] In the thermodynamic mechanism, relatively small pores are formed so that the patina acts as a semipermeable membrane that allows H_2O, H^+, OH^-, and Pb^{2+} ions. In kinetic passivation, all of the ions can move freely through the pores so that when the flow of lead ions is sufficiently high, the reaction proceeds at the pore orifice near the electrolyte, thus resulting in electrode potentials close to −0.95 V.[24−28]

Accordingly, peak I can be attributed to the reduction of the semipermeable PbO patina, whereas the electrochemical processes II and III can be associated with the reduction of different layers of porous corrosion products. The electrochemical reduction of PbO to Pb can be described in terms of a topotactic solid state transformation of lead oxide to lead metal without a morphological disintegration, superimposed to reduction involving intermediate Pb^{2+} ions in solution phase further reduced to lead metal.[15−17] The formation of a gross permeable layer of corrosion products under burial conditions would explain the enhancement of the reduction signal at −0.95 V (peak II)

dx.doi.org/10.1021/ac200731q |Anal. Chem. XXXX, XXX, 000–000

observed in archeological lead. All of processes I−III can be, in principle, represented by means of the following equation:

$$PbO(s) + 2H^+(aq) + 2e^- \rightarrow Pb(s) + H_2O \quad (1)$$

The overlapping peaks IVa and IVb can be attributed to the electrochemical reduction of PbO_2 that is electrochemically generated at potentials above +1.0 V by the oxidation of the PbO patina (and also of the Pb^{2+} ions in solution[29]), as judged upon comparison of voltammograms for patinated lead with those for litharge-modified electrodes.[19] Accordingly, the ubiquitous peaks IVa and IVb are recorded in all lead samples. The formation of α- and β-PbO_2 and substoichiometric lead oxides[30,31] can explain the multiple peak profile observed for PbO_2-modified electrodes immersed in an acetate buffer. Remarkably, whereas in contemporary lead such peaks remain isolated in the positive region of potentials, in archeological lead, peaks IVa and IVb are followed by a weak peak at +0.75 V (peak V). This peak, which appears clearly marked in the voltammograms of PbO_2 blanks, in agreement with literature,[14,18] can be attributed to the reduction of PbO_n species formed as a result of the (slow) natural corrosion process occurring as a result of contact with the atmosphere and soil during a prolonged time. The electrochemical reduction of PbO_2 can be formulated as the following:

$$PbO_2(s) + 2xH^+(aq) + 2xe^- \rightarrow PbO_{2-x}(s) + xH_2O \quad (2)$$

where $(0.6 < x < 1)$.[24,32] The absence of PbO_2 in "young" patinas can be used as an authentication test for archeological lead because peak V is absent in voltammograms of contemporary lead and forgeries where lead has been eventually subjected to "accelerated" corrosion procedures. Upon scanning the potential in the positive direction, stripping oxidation peaks for antimony, arsenic, bismuth, and copper accompanies the stripping of lead in archeological lead, thus providing an additional criterion for authentication (see Supporting Information).[18]

Voltammetric Dating. Let us assume that the surface of the lead artifact is initially covered by a patina formed during its handling as a result of exposure to the atmospheric environment. This patina, mainly formed by litharge, will be referred to as base patina in the text that follows. Let us assume that the artifact was further exposed to prolonged, uniform corrosion so that an additional layer of corrosion products is formed; this is a situation that is probably operative for lead artifacts buried in buffered carbonate soils.[3] Accordingly, one can assume that the peak height (or the peak area) of process II (i_{II}) is representative, under fixed electrochemical conditions (electrolyte, potential scan rate, etc.), of the amount of corrosion layer plus base patina formed during the corrosion period under burial conditions. In turn, the height of peak I (i_I) would be representative of the amount of base patina. Then, one can assume the following:

$$\frac{i_{II}}{i_I} = K_3 \frac{y_{base} + y_{corr}}{y_{base}} = K_3\left(1 + \frac{y_{corr}}{y_{base}}\right) \quad (3)$$

where y_{corr} and y_{base} represent the mass of the corroded metal by surface unit during the prolonged corrosion process and that of the initial patination step, respectively.

Now, let us assume that the advance of the corrosion process is related to the archeological age of the object or, more precisely, to the time of corrosion, t. Assuming that the corrosion process is based on the local existence of an electrochemical cell which comprises a junction of metallic oxide to a metal surface and the oxygen/water couple, the corrosion rate follows the potential law given here:[3,33]

$$dy_{corr}/dt = K_2 y_{corr}^{\alpha} \quad (4)$$

Integration between $t = 0$, $y = 0$ and t, y yields the following equation:

$$y_{corr} = [K_2(1+\alpha)t]^{1/(1+\alpha)} \quad (5)$$

Because there is no possibility of control of the amount of sample transferred to the electrode in the one-touch experiments, only the peak current (or the peak area) ratios can be used for relative quantification purposes. Combining eqs 3 and 5 yields the following:

$$\frac{i_{II}}{i_I} = K_3\{1 + K_4[K_2(1+\alpha)t]^{1/(1+\alpha)}\} \quad (6)$$

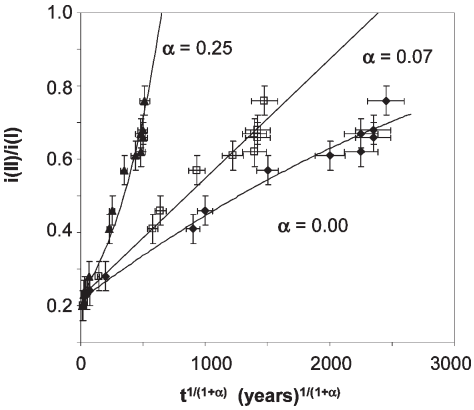

Figure 2. Plots of i_{II}/i_I vs $t^{1/(1+\alpha)}$ for contemporary lead and archeological samples in this study. From SWVs at graphite electrodes modified with the samples via one-touch methodology. Electrolyte 0.50 M HAc/NaAc, pH 4.85. Potential scan initiated at +1.25 V in the negative direction; potential step increment 4 mV; square wave amplitude 25 mV; frequency 5 Hz.

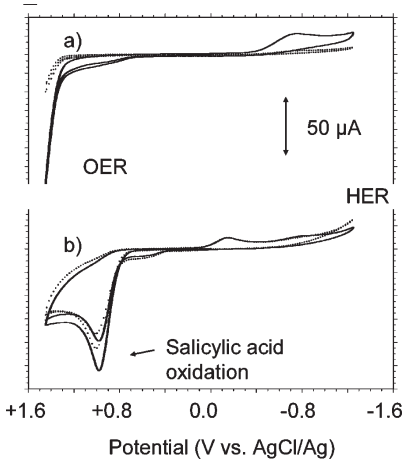

Figure 3. CVs for graphite electrodes modified by means of the one-touch methodology for contemporary lead (sample S.1 in the Supporting Information, dotted lines) and the archeological sample from the Tossal de Sant Miquel (sample S.12, continuous lines) immersed in (a) a 0.50 M potassium phosphate buffer with pH 7.00 and (b) a 5.0 mM salicylic acid solution in a 0.50 M potassium phosphate buffer with pH 7.00. The potential scan rate was 100 mV/s.

dx.doi.org/10.1021/ac200731q |Anal. Chem. XXXX, XXX, 000–000

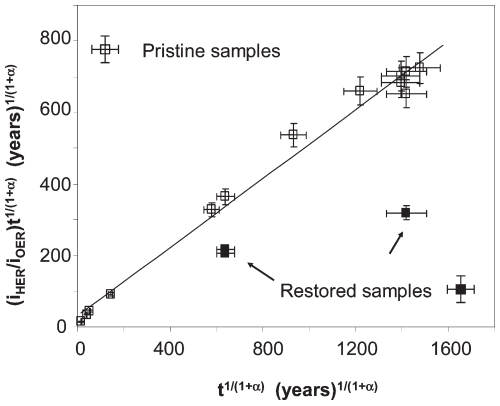

Figure 4. Plots of $(i_{HER}/i_{OER})t^{1/(1+\alpha)}$ vs $t^{1/(1+\alpha)}$ for samples in this study from CV data using conditions such as those in Figure 6.

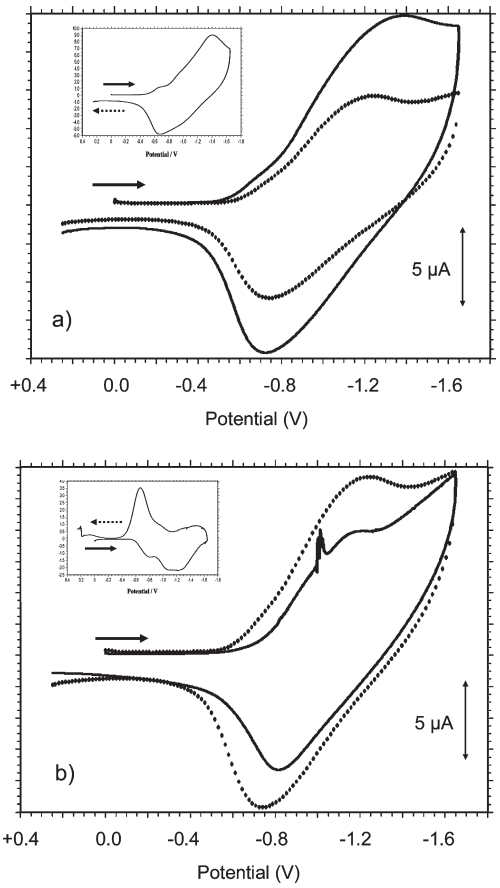

Figure 5. Comparison of deconvoluted CVs for air-saturated 0.10 M Bu_4NPF_6/MeCN at sample S.1 of contemporary lead (a, continuous line) and Visigothic sample S.10 (b, continuous line) attached to graphite bars using the one-touch sampling with the CV at the unmodified graphite electrode (a and b, dotted line). Potential scan rate 50 mV/s. Insets represent the corresponding subtracted current/potential curve. Arrows indicate the direction of the potential scan.

where $K_4 = K_3/y_{base}$. Assuming that the mass of young patina by surface unit, y_{base}, is essentially identical for all samples (vide infra), eq 6 predicts a linear relationship between the i_{II}/i_I ratio and $t^{1/(1+\alpha)}$ for the appropriate value of the coefficient α.

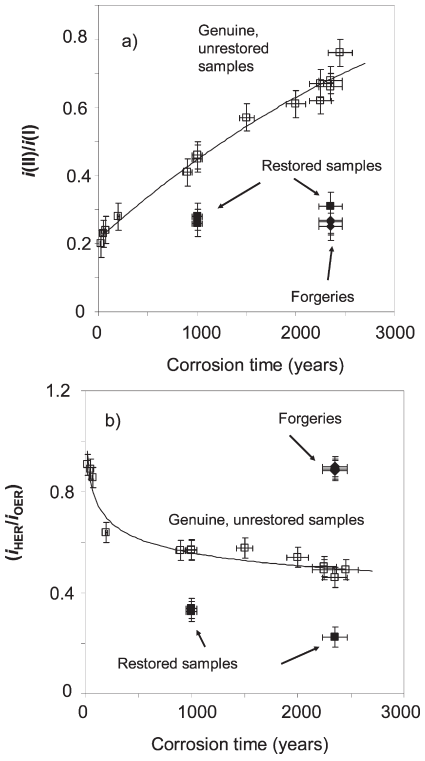

Figure 6. Variation of the (a) i_{II}/i_I ratio for SQWVs in acetate buffer and (b) i_{HER}/i_{OER} ratio for electrocatalytic CV experiments in a phosphate buffer with the corrosion time for genuine unrestored lead samples (squares), genuine restored samples (solid squares), and forgeries (solid rhombuses).

Figure 2 shows the representation of experimental i_{II}/i_I vs $t^{1/(1+\alpha)}$ for different α values. The best linear fit was obtained for α = 0.070, a value that is identical to that obtained by Reich et al.[3] using measurements on the Meissner fraction in the superconducting state of lead.

Electrocatalytic Dating. Electrocatalytic tests were performed to exploit the recognized catalytic ability of the involved materials. PbO_2 has been used as electrocatalytic material for different oxidation processes, in particular, the oxygen evolution reaction (OER),[34,35] whereas lead metal catalyzes the hydrogen evolution reaction (HER).[36−38] Under our experimental conditions, the relationship between the catalytic currents for HER and OER reactions could be representative of the PbO/PbO_2 ratio in the sample and, in turn, representative of the age of the piece. In Figure 3a shows the CVs obtained for contemporary lead and a sample from the Tossal de Sant Miquel (Iberian period, 2nd−4th century B.C.), immersed in a phosphate buffer at pH 7.00. Consistent with the aforementioned growing presence of PbO_2 in aged lead, the current above +1.0 V for OER is enhanced in archeological lead with respect to that for contemporary lead, while the HER current at −1.0 V exhibits the inverse variation. This last feature can be attributed to the blocking effect exerted by the corrosion patina on the catalytic activity of the metal.

Repeatability tests, however, produced 5−10% standard deviation in the quotient between the extreme currents for the HER and OER reactions, i_{HER}/i_{OER}. Interestingly, the repeatability was significantly increased (standard deviations ranging 2−5%) by introducing a radical scavenger, salicylic acid, whose oxidation precedes the OER (see Figure 3b). This possibly is due to its

dx.doi.org/10.1021/ac200731q |*Anal. Chem.* XXXX, XXX, 000–000

reaction with adsorbable $OH^{\bullet}$, which causes a decrease of the anodic generation of O_2.[37,39]

Under fixed electrochemical conditions, the i_{HER}/i_{OER} ratio should be representative of the quotient between the amount of PbO_2 generated during the corrosion process and the total lead (the parent deposit plus that electrochemically generated by reduction of lead oxides) accumulated in the electrochemical run. Under the previous assumptions one can write the following:

$$\left(\frac{i_{HER}}{i_{OER}}\right) = A\frac{1 + kt^{1/(1+\alpha)}}{kt^{1/(1+\alpha)}} \quad (7)$$

This equation predicts a linear dependence between $(i_{HER}/i_{OER})t^{1/(1+\alpha)}$ and $t^{1/(1+\alpha)}$. Experimental data are shown in Figure 4. It should be emphasized that, in spite of data dispersion, unrestored samples used for calibration can be fitted to a linear $(i_{HER}/i_{OER})t^{1/(1+\alpha)}$ vs $t^{1/(1+\alpha)}$ plot. Remarkably, the best fit of experimental data is obtained for $\alpha = 0.070$.

A complementary method to characterize pristine archeological lead can be obtained using the voltammetric responses associated with the electrochemical reduction of O_2 in nonaqueous solvents. This is a well-known electrochemical process consisting of a one-electron reversible reduction leading to $O_2^{\bullet -}$ radical anion which, in the presence of water traces, is followed by subsequent oxidation of the superoxide radical anion to hydroperoxyde and hydroxide anions.[40,41] For our purposes, the relevant point to emphasize is that this electrochemical process provides an in situ method for generating reactive radicals, which then influence the electrochemical response of the electrode, in particular, its electrocatalytic behavior, as recently reported by Scholz et al.[42−44] Following this line of reasoning, one can expect that the O_2 to $O_2^{\bullet -}$ reduction process at lead-modified electrodes can be influenced by the nature of the modifier and that, conversely, the catalytic ability of the patinated metal can be modified as a result of the generation of radicals on its surface. Figure 5 compares the CVs recorded at an unmodified electrode (dotted lines in parts a and b), for contemporary lead (continuous line in part a) and sample S.10 (continuous line in part b) immersed into air-saturated 0.10 M Bu_4NPF_6/MeCN. While contemporary lead moderately enhances both the cathodic and anodic peaks for the $O_2/O_2^{\bullet -}$ couple, all archeological samples display the opposite effect on this process. Such differences cannot be attributed to possible variations in the effective surface area of the graphite electrode resulting from its scratching, because this should be similar for the contemporary and archeological lead. Although no detailed mechanistic studies of the reduction of O_2 dissolved in organic solvents at lead are available, Pavlov et al.[45,46] have reported that the kinetics of the equivalent process in aqueous media is controlled by oxygen diffusion through the thin liquid film covering microparticulate deposits and impeded charge transfer through the electric double layer. On the basis of these results it appears reasonable to attribute the differences in the voltammetric response for contemporary and archeological lead with regard to the O_2 reduction to the corresponding differences in the texture and porosity of the corrosion patina covering lead metal.

Calibration. The dating of archeological lead from voltammetric data can be obtained from calibration curves using the parameters introduced in the precedent sections. Figure 6 compares the variation with the corrosion time of the i_{II}/i_I ratio for SQWVs in acetate buffer, shown in part a, with the i_{HER}/i_{OER} ratio for electrocatalytic CV experiments in a phosphate buffer for genuine unrestored lead samples, genuine restored samples, and forgeries, shown in part b. Data points for genuine unrestored lead samples for both the i_{II}/i_I and the i_{HER}/i_{OER} ratios can be satisfactorily represented by eqs 6 and 7, respectively, using $\alpha = 0.070 \pm 0.005$, which is a value in agreement with the results of Reich et al.[3] Remarkably, data points for genuine restored samples fall in regions clearly separated from the above. Similarly, using the corrosion time corresponding to the archeological site where the forgeries were found, data points for these samples fall far from those for genuine unrestored lead samples.

For both the i_{II}/i_I) and i_{HER}/i_{OER} ratios, experimental data points define an apparent continuous variation of the respective peak current ratios with the corrosion time, thus defining reasonable calibration curves for dating purposes. It should be noted, however, that the electrochemical dating described here is conditioned to the validity of the previously indicated simplifying assumptions.

The uncertainty in time measurements, Δt, can be related to both the uncertainty in the peak current ratio measurement, Δr ($r = i_{II}/i_I$), and the uncertainty in the α exponent, $\Delta\alpha$, which is in turn related to the analysis of the calibration data. Using the usual development of the theory of error propagation, one can obtain the relative uncertainty in the time derived from the potential relationship expressed by eq 8:

$$\frac{\Delta t}{t} = \frac{K_3\{1 + K_4[K_2\beta t]^{1/\beta}\}(\Delta r/r) + K_4[K_2\beta^{-(1+2\alpha)/\beta}t^{1/\beta}][\ln t - \ln\beta + \beta\ln k - 1](\Delta\alpha/\alpha)}{\beta^{-\alpha/\beta}K_4[K_2 t]^{(1+1\alpha)}} \quad (8)$$

where $\beta = 1 + \alpha$. Similarly, for eq 7, introducing the uncertainty in the i_{HER}/i_{OER} ratio, Δs, one can obtain the following:

$$\frac{\Delta t}{t} = (1+\alpha)(1 + kt^{1/1+\alpha})\left(\frac{\Delta s}{s}\right) + \frac{\alpha \ln t}{1+\alpha}\left(\frac{\Delta\alpha}{\alpha}\right) \quad (9)$$

According to the above expressions, and using parameters from calibration lines in Figures 2 ($\alpha = 0.070 \pm 0.005$; $K_3 = 0.223 \pm 0.015$; $K_4K_2^{0.935} = (3.25 \pm 0.15) \times 10^{-4}$) and 4 ($A = 0.481 \pm 0.016$; $k = 0.016 \pm 0.002$), the variation of the relative uncertainty in time measurement, $\Delta t/t$, can be estimated from the relative uncertainty of the i_{II}/i_I and i_{HER}/i_{OER} ratios and that for α, $\Delta\alpha/\alpha$. Theoretical calculations using the above parameters yield to age-dependent uncertainties in corrosion time measurement which reach values of ca. ±150 years for the more ancient samples in this study, similar to those usually handled in archaeometry.

CONCLUSIONS

The application of the voltammetry of microparticles to nanosamples from lead artifacts produces specific signatures for archeological lead, in particular, characteristic reduction signals for PbO_n and porous PbO formed during the corrosion process under burial conditions. Peak current ratios using the voltammetric peaks recorded for lead samples in contact with aqueous acetate buffer exhibit systematic variations with the time of corrosion for a series of lead samples that proceed from different archeological sites in the Valencia region (Spain).

Electrocatalytic currents for the hydrogen evolution and oxygen evolution reactions in an aqueous phosphate buffer also

dx.doi.org/10.1021/ac200731q |Anal. Chem. XXXX, XXX, 000–000

provide systematic variations with the corrosion time. The dating of the lead pieces can be obtained from such data by assuming that uniform environmental conditions acted during their corrosion process. For the studied set of samples, the potential law holds for the formation of PbO and PbO_2 during the corrosion process. It should be noted, however, that the proposed methodology is restricted to sets of samples with similar composition and conditions of aging.

In spite of the limitations associated with the simplifying assumptions introduced for electrochemical lead dating, the proposed methodology can provide a reasonable approach for establishing a systematic chronology of lead artifacts.

■ ASSOCIATED CONTENT

Supporting Information. Data summary of samples, photographs, experimental details, and additional figures. This material is available free of charge via the Internet at http://pubs.acs.org.

■ AUTHOR INFORMATION

Corresponding Author
*E-mail:antonio.domenech@uv.es.

■ ACKNOWLEDGMENT

We gratefully acknowledge the financial backing from the Spanish "I+D+I MEC" projects CTQ2006-15672-C05-05/BQU, CTQ2008-06727-C03-01/BQU, and 02/BQU (ERDF funds).

■ REFERENCES

(1) Aitken, M. J. *Science-Based Dating in Archaeology*; Longman: New York, 1990; Chapter 8.
(2) Renfrew, C.; Bahn, P. *Archaeology: Theory, Methods and Practice*; Thames & Hudson: London, 1991; Chapter 4.
(3) Reich, S.; Leitus, G.; Shalev, S. *New J. Phys.* **2003**, *5*, 99.1–99.9.
(4) Friedman, I.; Smith, R. L. *Am. Antiq.* **1960**, *25*, 476–493.
(5) Scholz, F.; Schröder, U.; Meyer, S.; Brainina, Kh. Z.; Zakharchuk, N. F.; Sobolev, N. V.; Kozmenko, O. A. *J. Electroanal. Chem.* **1995**, *385*, 139–142.
(6) Scholz , F.; Meyer, B. *Electroanalytical Chemistry: A Series of Advances*; Marcel Dekker, Inc.: New York, 1998; Vol. 20, pp 1−86.
(7) Scholz, F.; Schröder, U.; Gulabowski, R. *Electrochemistry of Immobilized Particles and Droplets*; Springer: Berlin, 2005.
(8) Doménech, A.; Doménech, M. T.; Costa, V. *Electrochemical Methods in Archaeometry, Conservation and Restoration*; Springer: Berlin, 2009.
(9) Doménech, A. *J. Solid State Electrochem.* **2010**, *14* (3), 349–351.
(10) Blum, D.; Leyffer, W.; Holze, R. *Electroanalysis* **1996**, *8*, 296–297.
(11) Costa, V.; Dubus, M. . In *Museum Microclimates*; Padfield, T., Ed.; The National Museum of Denmark: 2007; pp 63−65.
(12) Pernicka, E. *Jahrb. Romish-Germanishen Zentralmuseums* **1987**, *34*, 607–714.
(13) Blaskett, D. R.; Boxall, O. *Lead and its Alloys*; Ellis Horwood: London, 1990.
(14) Zakharchuk, N.; Meyer, S.; Lange, B.; Scholz, F. *Croat. Chem. Acta* **2000**, *73*, 667–704.
(15) Meyer, B.; Ziemer, B.; Scholz, F. *J. Electroanal. Chem.* **1995**, *392*, 79–83.
(16) Hasse, U.; Scholz, F. *Electrochem. Commun.* **2001**, *3*, 429–434.
(17) Doménech, A.; Doménech, M. T.; Mas, X. *Talanta* **2007**, *71*, 1569–1579.
(18) Doménech, A. Doménech, M. T. Peiró, M. A. Osete, L. *Electroanalysis* **2011** [Online early access]. DOI: 10.1002/elan.201000739. Published Online: May 17, 2011.
(19) Doménech, A. Doménech, M. T. Peiró, M. A. *Arcaheometry* **2011** [Online early access]. DOI: 10.1111/j.1475-4754.2011.00608.x. Published Online: May 27, 2011.
(20) Sandu, I.; Marutoiu, C.; Sandu, I. G.; Alexandru, A.; Sandu, A. V. *Acta Univ. Cibiniensis, Ser. F: Chem.* **2006**, *9*, 39–53.
(21) Tétreault, J.; Cano, E.; Van Bommel, M.; Scott, D.; Dennis, M. *Stud. Conserv.* **2003**, *48*, 237–250.
(22) Degrigny, C. *J. Solid State Electrochem.* **2010**, *14*, 353–361.
(23) Cano, E.; Lafuente, D.; Bastidas, D. M. *J. Solid State Electrochem.* **2010**, *14*, 381–391.
(24) Pavlov, D. *Electrochim. Acta* **1968**, *13*, 2051–2061.
(25) Pavlov, D.; Popoda, R. *Electrochim. Acta* **1970**, *15*, 1483–1491.
(26) Pavlov, D.; Monakhov, B. *J. Electroanal. Chem.* **1987**, *218*, 135–153.
(27) Pavlov, D.; Monakhov, B.; Salmi, K.; Sundholm, G. *Electrochim. Acta* **1991**, *36*, 953–963.
(28) Cai, W.-B.; Wan, Y.-Q.; Liu, H.-T.; Zhou, W.-F. *J. Electroanal. Chem.* **1995**, *387*, 95–100.
(29) Laitinen, H. A.; Watkins, N. H. *Anal. Chem.* **1975**, *47*, 1352–1358.
(30) Pavlov, D. *J. Electroanal. Chem.* **1981**, *118*, 167–185.
(31) Bartlett, P. N.; Dunford, T.; Ghanem, M. A. *J. Mater. Chem.* **2002**, *12*, 3130–3135.
(32) Pavlov, D.; Monakhov, B. *J. Electrochem. Soc.* **1989**, *136*, 27–33.
(33) Chilton, J. P. *Principles of Metallic Corrosion*; The Royal Institute of Chemistry: London, 1968.
(34) Zhao, G.; Zang, Y.; Lei, Y.; Lv, B.; Gao, J.; Zhang, Y.; Li, D. *Environ. Sci. Technol.* **2010**, *44*, 1754–1759.
(35) Rodgers, J. D.; Jedral, W.; Bunce, N. J. *Environ. Sci. Technol.* **1999**, *33*, 1453–1457.
(36) Gopalakrishna, M.; Rao, M.; Smith, F. R. *J. Chem. Soc., Chem. Commun.* **1972**, 266–268.
(37) Panizza, M.; Cerisola, G. *Electrochim. Acta* **2003**, *48*, 3491–3497.
(38) Wu, Y. M.; Li, W. S.; Long, X. M.; Wu, F. H.; Chen, H. Y.; Yan, J. H.; Zhang, C. R. *J. Power Sources* **2005**, *144*, 338–345.
(39) Ai, S.; Wang, Q.; Li, H.; Jin, L. *J. Electroanal. Chem.* **2005**, *578*, 223–229.
(40) Cofré, P.; Sawyer, D. T. *Anal. Chem.* **1986**, *58*, 1057–1062.
(41) Singh, P. S.; Evans, D. H. *J. Phys. Chem. B* **2006**, *110*, 637–644.
(42) Scholz, F.; López de Lara González, G.; Machado de Carvalho, L.; Hilgemann, M.; Brainina, Kh. Z.; Kahlert, H.; Jack, R. S.; Minh, D. T. *Angew. Chem.* **2007**, *119*, 8225–8227.
(43) Scholz, F.; López de Lara González, G.; Machado de Carvalho, L.; Hilgemann, M.; Brainina, Kh. Z.; Kahlert, H.; Jack, R. S.; Minh, D. T. *Angew. Chem., Int. Ed.* **2007**, *46*, 8079–8081.
(44) Nowicka, A.; Hasse, U.; Sievers, G.; Donten, M.; Stojek, Z.; Fletcher, S.; Scholz, F. *Angew. Chem., Int. Ed.* **2010**, *49*, 3006–3009.
(45) Kirchev, A.; Pavlov, D.; Monahov, B. *J. Power Sources* **2003**, *113*, 245–254.
(46) Pavlov, D.; Kirchev, A.; Monahov, B. *J. Power Sources* **2005**, *144*, 521–527.